THE JOURNAL OF PHYSIOLOGY

The compliance of the porcine pulmonary artery depends on pressure and heart rate

L. Kornet, J. R. C. Jansen, F. C. A. M. te Nijenhuis, G. J. Langewouters and A. Versprille

J. Physiol. 1998;512;917-926

The compliance of the porcine pulmonary artery depends on pressure and heart rate

L. Kornet, J. R. C. Jansen, F. C. A. M. te Nijenhuis, G. J. Langewouters* and A. Versprille

*Pathophysiological Laboratory, Department of Pulmonary Diseases, Erasmus University, Rotterdam and *TNO Biomedical Instrumentation, Academic Medical Centre, Amsterdam, The Netherlands*

(Received 23 February 1998; accepted after revision 29 July 1998)

1. The influence of mean pulmonary arterial pressure (mean P_{pa}) on dynamic (C_d) and pseudo-static compliance (C_{ps}) of the pulmonary artery was studied at a constant and a changing heart rate. C_d is the change in cross-sectional area (CSA) relative to the change in P_{pa} throughout a heart cycle. C_{ps} is the change in mean CSA relative to the change in mean P_{pa}. If C_d is known, pulmonary blood flow can be computed from the P_{pa} using a windkessel model. We investigated whether C_{ps} can be interchanged with C_d.

2. In nine anaesthetized pigs, we determined the mean CSA and C_d of the pulmonary artery at various P_{pa} levels, ranging from approximately 30 to 10 mmHg, established by bleeding. Two series of measurements were carried out, one series at a spontaneously changing heart rate ($n = 9$) and one series at a constant heart rate ($n = 6$). To determine CSA a conductance method was used.

3. C_{ps} depended on pressure. The mean CSA *versus* mean P_{pa} curves were sigmoid and steepest in the series with the increasing heart rate (established by bleeding). The CSA *versus* P_{pa} loop during a heart cycle, giving C_d, was approximately linear and almost closed. The C_d *versus* mean P_{pa} relationship was bell shaped. Its width was smaller if the heart rate increased during the series of measurements. The pressure, where C_d was maximum, was higher at higher heart rates. Furthermore, the maximum C_d was not affected by the heart rate.

4. Because the pulmonary artery constricts with increasing heart rate, C_{ps} will be over-estimated during procedures where heart rate increases. C_d should be determined on a beat-to-beat basis to calculate flow because it changes with mean pulmonary arterial pressure and heart rate.

Pulmonary flow can be derived from a pulmonary arterial pressure curve for patients for which this pressure is routinely determined, such as patients who are undergoing intensive care, cardio-thoracic surgery or a catheterization for diagnostic reasons, without the use of a flow probe. To compute the pulmonary blood flow beat-to-beat for a specific haemodynamic condition from the arterial pressure curve a windkessel model should be used. To do so, the dynamic compliance of the pulmonary artery under the specified haemodynamic condition must first be known. Dynamic compliance is the change in cross-sectional area (CSA) related to the change in pulmonary arterial pressure (P_{pa}) during a heart beat. Static compliance is the change in mean CSA related to the change in mean P_{pa}. We define static compliance measured *in vivo* as pseudo-static compliance, because the pressure and CSA fluctuate cyclically during one heart beat.

In most of the literature on vessel compliance no distinction is made between static, pseudo-static and dynamic compliance, e.g. instead of dynamic compliance the static compliance, as obtained from *in vitro* experiments (Langewouters, 1984), was used for the aorta to compute aortic blood flow (Jansen *et al.* 1990; Weissman *et al.* 1993; Wesseling *et al.* 1993). This is only valid if creep is negligible and no influence of pressure and heart rate is present. Various authors have found that the creep of the pulmonary artery is indeed negligible (Patel *et al.* 1960; Greenfield & Griggs, 1963; Ingram *et al.* 1970; Shelton & Olson, 1972; Gozna *et al.* 1974; Johnson & Henry, 1985). They have also found a constant dynamic compliance over a limited range of pulmonary arterial pressure. However, other authors predicted an influence of pressure on dynamic compliance if windkessel models were used to describe the pulmonary arterial circulation (Grant *et al.* 1991; Lieber *et*

al. 1994). Furthermore, it has been suggested that heart rate is a major determinant of aortic compliance (Marcus *et al.* 1994). Accordingly, aortic compliance has been adjusted for pressure and heart rate to compute aortic blood flow beat-to-beat from the aortic pressure, using windkessel models (Jansen *et al.* 1990; Weissman *et al.* 1993; Wesseling *et al.* 1993).

We studied the influence of pressure and heart rate on compliance in anaesthetized pigs by comparing the relationship between the mean CSA and the mean pulmonary arterial pressure obtained over a large pressure range under conditions of spontaneously changing heart rate with that obtained at a constant heart rate. We also investigated whether the dynamic compliance of the pulmonary artery is constant during a cardiac cycle and we compared the relationship between dynamic compliance and mean pulmonary arterial pressure in both series. CSA was determined using a conductance method (Baan *et al.* 1984).

METHODS

Surgical procedures and ventilatory conditions

All experiments were performed in accordance with the *Guide for Care and Use of Laboratory Animals* published by the US National Institutes of Health (NIH publication No. 85-23, revised 1985) and in accordance with the regulations of the Animal Care Committee of Erasmus University.

Nine piglets (5–7 weeks old, $12{\cdot}0 \pm 1{\cdot}3$ kg body weight) were anaesthetized with an intraperitoneal injection of pentobarbital sodium (30 mg (kg body weight)$^{-1}$). The animals were placed in a supine position on a thermo-controlled operating table to maintain body temperature at about 38·5 °C. Anaesthesia was maintained by a continuous infusion of pentobarbital sodium (8·5 mg kg^{-1} h^{-1}) via an ear vein. ECG electrodes were placed subcutaneously in the right leg and on the chest near the xyphoid cartilage. After tracheotomy, the pigs were connected to a volume-controlled ventilator (Jansen *et al.* 1989) and ventilated with ambient air. The ventilatory rate was set at ten breaths per minute. Tidal volume was adjusted to a P_{a,CO_2} of 38–42 mmHg during baseline. The ratio of inspiration to expiration was 2 : 3 times. A positive end-expiratory pressure of 2 cmH_2O was applied.

A catheter was inserted through the right common carotid artery into the aortic arch to measure the arterial pressure and to sample the blood. A four-lumen catheter was inserted via the right external jugular vein into the superior vena cava to measure the central venous pressure, to inject a hypertonic salt solution and to infuse pentobarbital and pancuronium. After thoracotomy at the left site of the sternum, a catheter surrounded by a fluid-filled sheet for measuring the pressure was inserted through the right ventricular wall into the pulmonary artery to measure the electrical conductance and the temperature of the pulmonary arterial blood (Fig. 1). The pressure transducer was located only 10 cm from the site of measurement, to avoid damping of the pressure signal by the fluid-filled sheet (Fig. 1). All conductance catheter electrodes were positioned in the pulmonary trunk with the proximal electrode downstream from the pulmonary valve and outside the sheet. The thorax remained open during the experiment. Therefore, the pulmonary arterial pressure was equal to the transmural wall pressure. A pacemaker electrode was fixed to the right auricle.

To avoid clotting in the catheters, the three pressure catheters were continuously flushed at a flow rate of 3 ml h^{-1} with saline (0·9% NaCl) containing 10 i.u. heparin ml^{-1}. A catheter was placed in the bladder to prevent retention of urine. After the surgical procedures, pancuronium bromide (0·3 mg kg^{-1} h^{-1}, after a loading dose of 0·2 mg kg^{-1}) was given intravenously to suppress spontaneous breathing. The pentobarbital infusion was switched from the ear vein to the vena cava superior. The surgical procedures were followed by a stabilization period of about half an hour.

Conductance method

To determine the cross-sectional area (CSA) of the pulmonary artery, we modified the intraventricular conductance method (Baan *et al.* 1984). Only the essentials will be presented in this paper. The catheter has four electrodes equidistantly (5 mm) placed at its distal end. An alternating current of 70 μA (r.m.s.) and 20 kHz was applied to the two outer electrodes (model Sigma 5, Leycom, Cardiodynamics, Rijnsburg, The Netherlands). The induced voltage was measured at the two inner electrodes. An offset was caused by the conductance of the surrounding tissues, which is called parallel conductance. The cross-sectional area, which varies with time (CSA(t); mm^2), is related to the measured conductance area, which varies with time ($G(t)$; 1/Ω), by the relationship:

$$\mathrm{CSA}(t) = \frac{L}{\sigma_b(t)}(G(t) - G_p), \tag{1}$$

where L is the distance between the electrodes (mm), $\sigma_b(t)$ the electrical conductivity of the flowing blood (1/(Ω × mm)) and G_p the parallel conductance (1/Ω).

G_p is determined by changing the conductivity of blood using saline injections (Baan *et al.* 1984). During passage of a hypertonic salt concentration, conductance gradually increases and decreases as a dilution curve. During the increase in the specific conductivity of

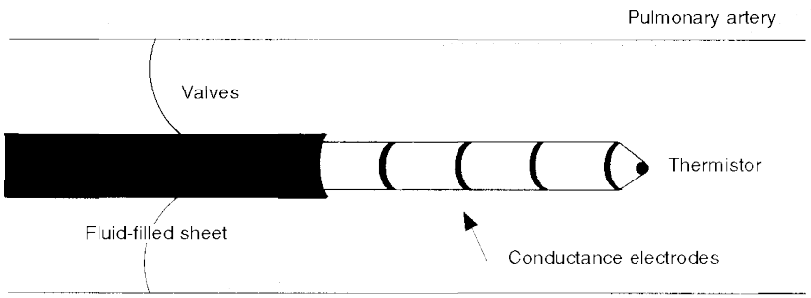

Figure 1. Diagram of the conductance catheter situated in the pulmonary artery

blood only, a series of paired G_{sys} (conductance at systole) and G_{dias} (conductance at diastole) values were obtained. If the linear regression line through these values was extrapolated to the point where the conductivity of blood was zero, $G_{sys} = G_{dias} = G_p$.

In vitro experiments revealed that the conductivity of stagnant blood ($\sigma_{b(static)}$; $1/(\Omega \times cm)$) depends on the temperature (T; °C) and the haematocrit (Ht; %) according to:

$$\sigma_{b(static)} = (-1{\cdot}17 \times 10^{-4})Ht + (2{\cdot}33 \times 10^{-4})T - (3{\cdot}82 \times 10^{-6})HtT + (6{\cdot}65 \times 10^{-3}). \quad (2)$$

The Pearson correlation coefficient of this multiple regression is 0·9998. This conductivity needs to be corrected for the shear rate caused by blood flow, which leads to orientation and deformation of erythrocytes (Sakamoto & Kanai, 1979). The maximum effect of shear rate on conductivity was found above a shear rate of 13 s^{-1}, averaged across the CSA of the glass tube. The maximum effect of shear rate on the percentage increase in conductivity ($\Delta\sigma_b$) related to percentage haematocrit according to:

$$\Delta\sigma_b = 0{\cdot}5(\Delta\sigma_{max} + \Delta\sigma_{max}(1 - e^{-K|Ht-X50|})sign(Ht - X50)), \quad (3)$$

with the following fit variables:

$$X50 = 38{\cdot}20 \pm 0{\cdot}42,$$

$$K = 0{\cdot}16 \pm 0{\cdot}01,$$

$$\Delta\sigma_{max} = 16{\cdot}48 \pm 0{\cdot}67,$$

where X50 is the percentage haematocrit at the steepest slope of the relationship, K the steepness of the fit, calculated as the percentage increase in conductivity divided by the percentage haematocrit, and $\Delta\sigma_{max}$ the maximum increase in conductivity as a percentage. Sign(Ht − X50) is +1 if the haematocrit is larger than 38%, −1 if the haematocrit is smaller than 38% and 0 if the haematocrit equals 38%.

Maximum shear rate is exceeded almost throughout systole (Sømod *et al.* 1993), particularly if a catheter is positioned in the vessel. We found that erythrocytes orientate almost instantaneously and de-orientate and reform in 240 ± 40 ms which is longer than the diastolic period for the animals described in this paper. Therefore, to obtain the conductivity of flowing blood (σ_b), the conductivity of stagnant blood ($\sigma_{b(static)}$) was multiplied by a constant correction factor for the influence of shear rate (F_{SR}) throughout the heart cycle according to the equation:

$$F_{SR} = 1 + \Delta\sigma_{b(static)}/100. \quad (4)$$

We evaluated the conductance method in the aorta of five piglets using an intravascular ultrasound method. The regression line through the cross-sectional areas determined with the conductance method (CSA_G) *versus* those determined using the intravascular ultrasound method (CSA_{IVUS}) was close to the line of identity ($CSA_G = -0{\cdot}086 + 0{\cdot}999 \times CSA_{IVUS}$, $r = 0{\cdot}97$). The difference in CSAs was independent of the diameter of the vessel and was on average $-0{\cdot}11 \pm 2{\cdot}79$ mm^2 (mean ± S.D.). We therefore considered the conductance method applicable for our study.

Experimental protocol

Using nine animals, we carried out a series of observations at a spontaneously changing heart rate, followed by a second series in six of these animals carried out at a constant heart rate; this heart rate was about equal to the highest value of the first series. Before each series, parallel conductance (G_p) was determined from the data obtained after three injections of a hypertonic salt solution (5 ml, 3 M), each injected during an expiratory pause of 12 s. During both series, mean pulmonary arterial pressure was changed by decreasing blood volume by 10–20 ml every 3 min. This bleeding procedure was stopped at an aortic pressure of approximately 40 mmHg. Shortly before each bleeding, 0·5 ml blood was sampled to determine haematocrit. Next, pulmonary arterial pressure, blood temperature and electrical conductance signals were sampled during an expiratory pause of 12 s at a frequency of 250 Hz. The signals were stored on a hard disk for off-line analysis. After each series, all blood extracted during the bleeding steps was slowly reinfused. At the end of the experiments the animals were killed with an overdose of pentobarbital.

Calculations

Haemodynamic variables, such as pulmonary arterial pressure, venous pressure, aortic pressure, heart rate and CSA, were determined under normovolaemic baseline conditions and after maximal bleeding. Each of the variables was averaged over all heart cycles for 5 s of an expiratory pause period. To calculate the mean CSA, eqns (1)–(4) were used.

Pseudo-static compliance (i.e. $C_{ps} = \Delta(\text{mean CSA})/\Delta(\text{mean } P_{pa})$) is the derivative of the relationship between the mean CSA *versus* the mean P_{pa}. Dynamic compliance (i.e. $C_d = \Delta CSA/\Delta P_{pa}$) is the slope of the linear regression line through the CSA *versus* pulmonary arterial pressure values during the heart cycles. Dynamic compliance can be determined without determining the parallel conductance, because parallel conductance only introduces an offset in the CSA signal. We used the dynamic compliance obtained from the whole heart cycle, using a factor to correct for the influence of shear rate. We assumed that the influence of shear rate is constant within a heart cycle. Data are presented as means ± S.D.

RESULTS

Haemodynamic data under normovolaemic baseline conditions and data after maximal bleeding are given for both experimental series in Table 1. Baseline heart rate is significantly higher in series 2 than in series 1. Mean pulmonary arterial pressure (mean P_{pa}) was significantly higher (Student's paired t test, $n = 6$, $P < 0{\cdot}05$, Fig. 2) and mean CSA significantly lower (paired t test, $n = 6$, $P < 0{\cdot}05$, Fig. 2) at the start of the second series at a high heart rate than the corresponding values at the start of the first series where the heart rate was low. Mean aortic pressure (mean P_{ao}) and mean central venous pressure (mean P_{cv}) were not significantly different (paired t test, $n = 6$, $P > 0{\cdot}05$). After maximal bleeding at the end of series 1 and at the end of series 2, no significant differences were found between mean P_{ao}, mean P_{pa}, mean P_{cv}, HR and mean CSA (paired t test, $n = 6$, $P > 0{\cdot}05$).

Because some de-orientation and shape recovery of erythrocytes might occur at the end of diastole, we studied whether such an effect of de-orientation and reformation at diastole caused a significant error in the determination of compliance obtained from the whole heart cycle. For this reason, compliances determined from systolic periods were compared with compliances determined from diastolic periods obtained during 5 s of an expiratory pause. A

Table 1. Haemodynamic variables

	Series 1 (at a changing heart rate)		Series 2 (at a constant heart rate)	
Variable	Baseline	Maximal bleeding	Baseline	Maximal bleeding
Mean P_{ao} (mmHg)	84·41 ± 9·36	38·96 ± 11·88	90·12 ± 9·44	42·11 ± 9·07
Mean P_{pa} (mmHg)	20·26 ± 5·60	11·00 ± 2·93	26·78 ± 3·99*	12·75 ± 2·99
Mean P_{cv} (mmHg)	4·25 ± 2·44	1·75 ± 1·57	6·04 ± 1·67	2·01 ± 1·63
HR (Hz)	2·17 ± 0·36	3·75 ± 0·43	3·85 ± 0·31	3·85 ± 0·31
Mean CSA (mm^2)	160·3 ± 34·4	104·1 ± 43·8	154·8 ± 36·7*	121·7 ± 38·1

For six experiments the haemodynamic variables are given for both series at baseline and after maximal bleeding: mean pulmonary arterial pressure (mean P_{pa}), mean aortic pressure (mean P_{ao}), mean central venous pressure (mean P_{cv}), heart rate (HR) and mean cross-sectional area (mean CSA). * Change is significant compared with the same volaemic condition in series 1.

systolic period was defined as the period from end-diastolic pressure to the incisura of the dicrotic notch of the peak systolic pressure. A diastolic period was defined as the period from the incisura of the dicrotic notch to the end-diastolic pressure. No significant difference existed between dynamic compliances determined during the systolic periods and those determined during the diastolic periods (95% confidence interval of mean difference $C_{d,systole} - C_{d,diastole} = 0{\cdot}007 \pm 0{\cdot}081$ mm^2 $mmHg^{-1}$, paired t test, $n = 227$). These findings support our previous conclusion that the effect of shear rate on conductivity can be considered constant during the whole heart cycle. The reason for this is the high heart rate in piglets.

Pseudo-static compliance

The mean pulmonary arterial CSA *versus* mean P_{pa} relationships measured at spontaneously changing and at constant heart rates are presented in Fig. 2. In all series each bleeding step caused a lower P_{pa} and a lower CSA. The shape of the CSA *versus* P_{pa} curve was sigmoid for both series. During series 1, the heart rate (HR) increased with successive bleeding steps. In all experiments the CSA *versus* pressure relationship was steeper for series 1 at an increasing heart rate than for series 2 at a constant heart rate. The largest change in CSA coincided with the largest change in HR. After reinfusion of blood the CSA and the heart rate returned to their normovolaemic baseline values.

To find the best mathematical description of the relationship between CSA and pressure, we fitted linear, exponential, hyperbolic and inverse tangent functions through the CSA *versus* pressure points using the least squares Marquardt method. In each experiment where the heart rate changed during bleeding, the exponential fit procedure gave the smallest sum squared error (Fig. 2*a–i*). In series 2, where the heart rate was constant, an exponential function was also used (Fig. 2*d–i*).

The equation of the exponential function to fit the CSA *versus* P_{pa} data is expressed:

$$\mathrm{CSA} = \mathrm{CSA}_{ps,0} + \frac{\mathrm{CSA}_{ps,1} - \mathrm{CSA}_{ps,0}}{1 + \exp\left(\dfrac{P_{ps,0} - P_{pa}}{P_{ps,1}}\right)}, \tag{5}$$

where $\mathrm{CSA}_{ps,0}$ is the minimum asymptotic CSA value (mm^2); $\mathrm{CSA}_{ps,1}$ the maximum asymptotic CSA value (mm^2); $P_{ps,0}$ the pressure (mmHg) where the CSA *versus* pressure curve is steepest and thus pseudo-static compliance is maximal, and $P_{ps,1}$ the difference between $P_{ps,0}$ and the pressure where the compliance is 79% of the maximum value ($0{\cdot}79 = \sqrt{0{\cdot}63} = \sqrt{\tau}$). The results of the fit are given in Fig. 2.

The derivative of the fit through the mean CSA *versus* mean pressure points ($\delta\mathrm{CSA}/\delta P$) is defined as the pseudo-static compliance (C_{ps}). Pseudo-static compliance *versus* mean P_{pa} relationships derived for both series, at spontaneously changing and constant heart rates, are presented in Fig. 3*Aa–i* above the dynamic compliance *versus* mean P_{pa} relationships of the corresponding experiments (Fig. 3*Ba–i*) to make comparison between both compliances easier. The derivative of the exponential fit (eqn (5)) is given as eqn (6):

$$C_{ps} = \frac{\dfrac{\mathrm{CSA}_{ps,1} - \mathrm{CSA}_{ps,0}}{P_{ps,1}} \exp\left(\dfrac{P_{ps,0} - P_{pa}}{P_{ps,1}}\right)}{1 + \exp\left(\dfrac{(P_{ps,0} - P_{pa})^2}{P_{ps,1}}\right)}. \tag{6}$$

For $P_{pa} = P_{ps,0}$ the equation becomes:

$$C_{ps,max} = \frac{\mathrm{CSA}_{ps,1} - \mathrm{CSA}_{ps,0}}{4P_{ps,1}}, \tag{7}$$

where $C_{ps,max}$ is the maximum pseudo-static compliance (mm^2 $mmHg^{-1}$).

Without intending to suggest a physiological relationship between heart rate and mean P_{pa}, we found an exponential relationship between heart rate and P_{pa} (series 1). This function is a mirror image of the function fitted through the CSA *versus* P_{pa} data (Fig. 2). The least squares Marquardt method was also used. The formula for the exponential function is expressed as:

$$HR = HR_0 - \frac{HR_1 - HR_0}{1 + \exp\left(\frac{P_{HR,0} - P_{pa}}{P_{HR,1}}\right)}, \quad (8)$$

where HR_0 and HR_1 are the maximum and minimum asymptotic heart rate values (Hz) respectively, $P_{HR,0}$ is the pulmonary arterial pressure (mmHg) where the HR *versus* pressure curve is steepest, and $P_{HR,1}$ the pressure difference between $P_{HR,0}$ and the pressure when the change in heart rate is 79% of the maximum change in heart rate. The maximal steepness of the heart rate ($S_{HR,max}$) *versus* pressure fit is given by:

$$S_{HR,max} = \frac{HR_0 - HR_1}{4P_{HR,1}}, \quad (9)$$

where $S_{HR,max}$ is expressed in (Hz mmHg^{-1}). The results of the fit are given in Fig. 2.

The maximum pseudo-static compliance, $C_{ps,max}$, correlated positively with the maximum decrease in heart rate ($r = 0{\cdot}83$, 95% confidence interval $= 0{\cdot}54$, $0{\cdot}95$, $n = 14$). The extreme increase in heart rate coinciding with the extreme pseudo-static compliance of the experiment shown in Fig. 2*d* was not considered. Furthermore, the linear regression line through the values of pressure when pseudo-static compliance was maximal *versus* the pressure when the change in heart rate was maximal did not deviate significantly from the line of identity (Fig. 4).

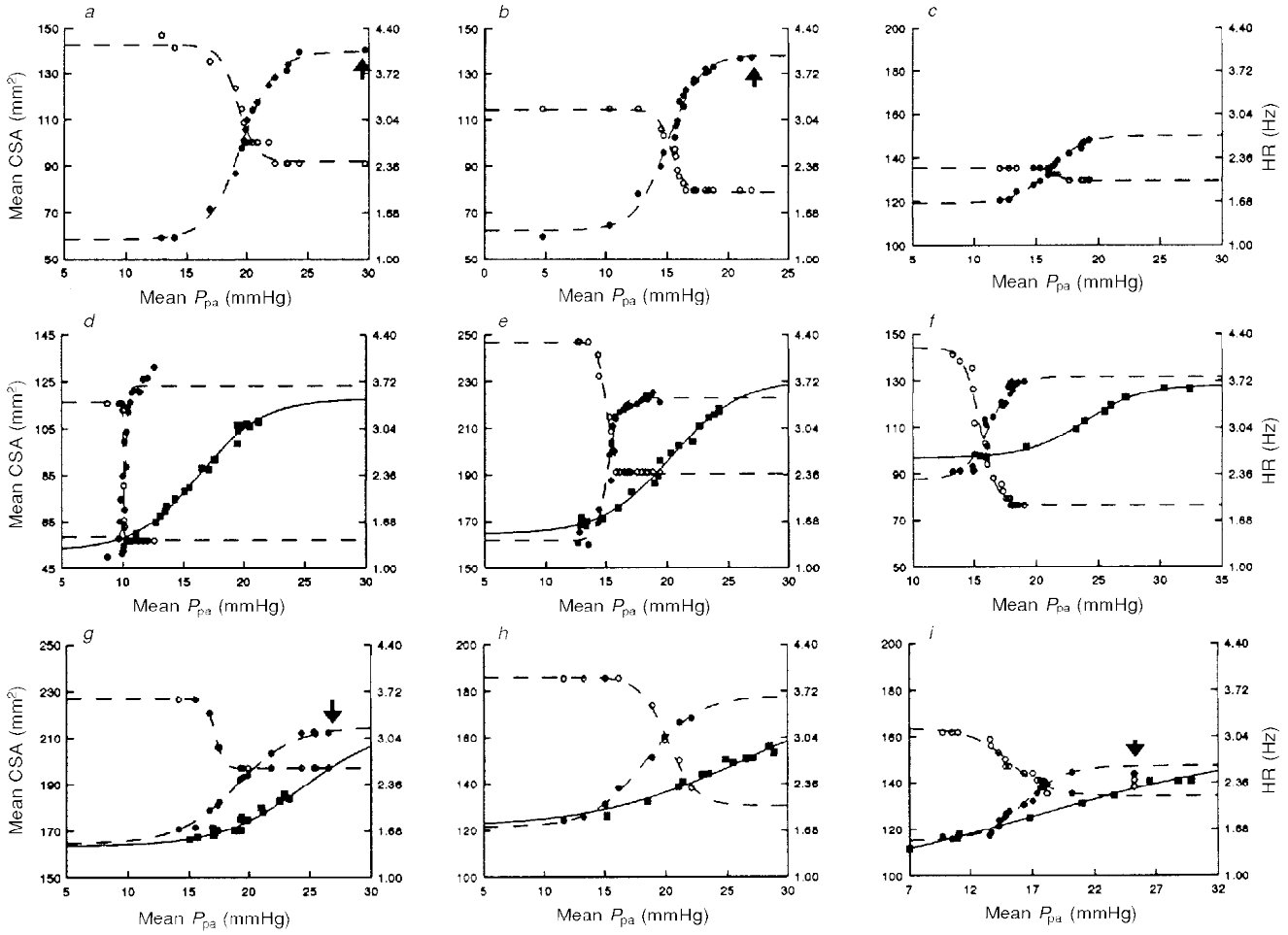

Figure 2. Mean CSA *versus* mean pressure

Mean pulmonary cross-sectional area (mean CSA) and heart rate (HR) are plotted on the left and right ordinates, respectively, against mean pulmonary arterial pressure (mean P_{pa}) on the abscissa. Two series of experiments were done in six (*d–i*) of the nine (*a–i*) animals. Closed symbols are the data points of CSA *vs.* mean P_{pa} for series 1 (●) and series 2 (■). Open symbols are the data points of HR *vs.* mean P_{pa} for series 1 (○). The arrows indicate data points obtained after reinfusion of blood. Fits are drawn through the CSA *versus* pressure points and through the heart rate *versus* pressure points.

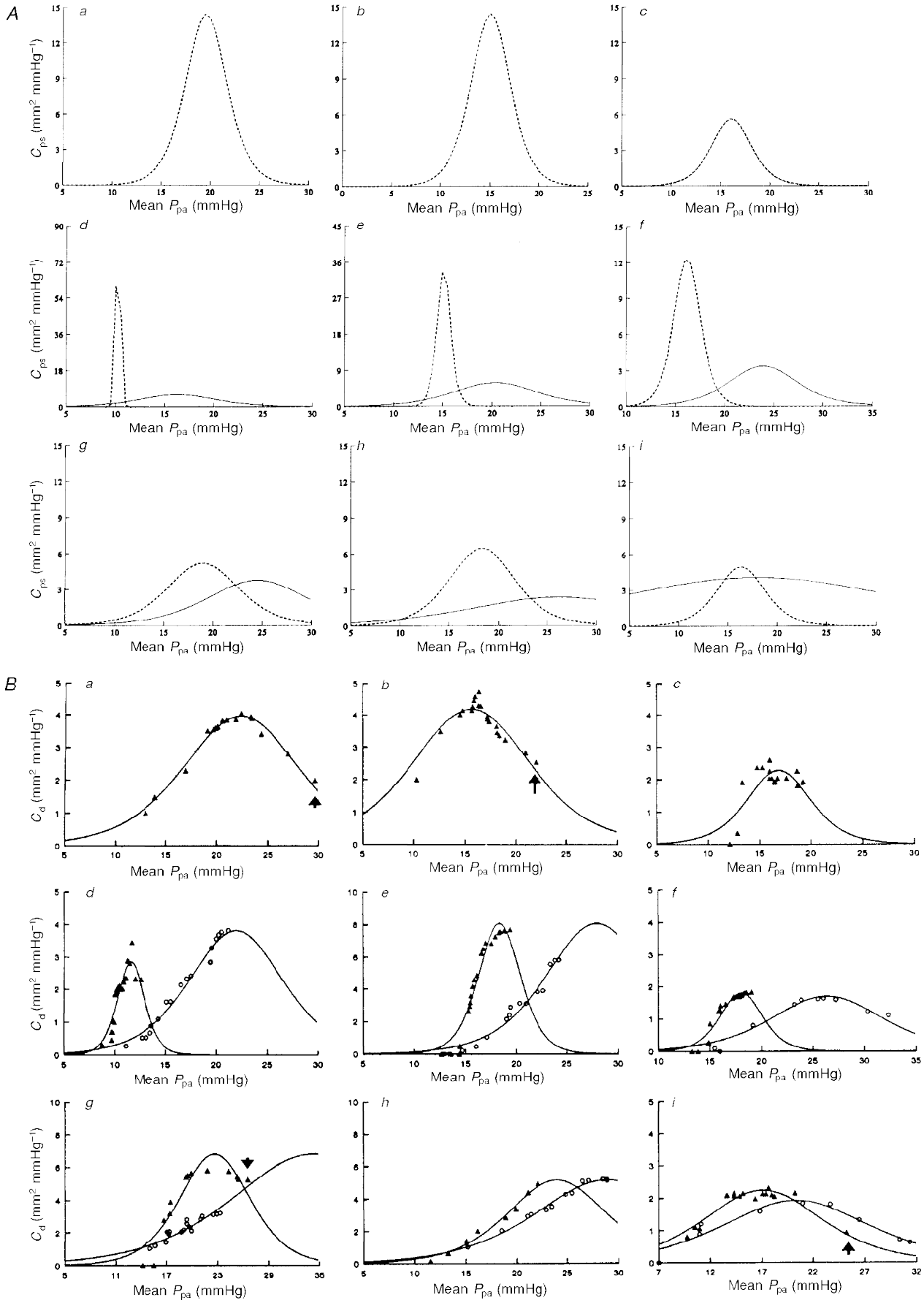

Figure 3. For legend see facing page.

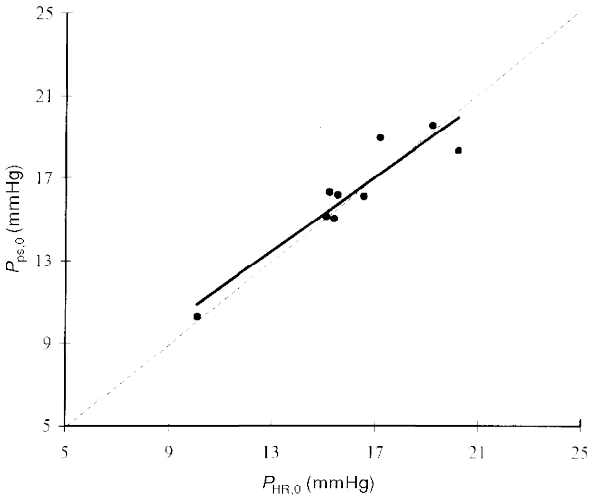

Figure 4
The graph plots the pressure when the change in pseudo-static compliance is maximal ($P_{ps,0}$) *versus* the pressure when the change in heart rate is maximal ($P_{HR,0}$).

Dynamic compliance

All loops of CSA *versus* P_{pa} within a heart cycle were almost closed and a linear regression line appeared to be the best fit through each individual loop. The loops coincided with the pseudo-static relationship of mean CSA *versus* mean P_{pa} at a constant heart rate (Fig. 5*B*), whereas they did not with the pseudo-static relationship at an increasing heart rate (Fig. 5*A*).

Individual plots of dynamic compliance *versus* mean pulmonary arterial pressure are given for both series in Fig. 3*Ba–i* below the plots of pseudo-static compliance *versus* mean pulmonary arterial pressure of the corresponding experiments (Fig. 3*Aa–i*). A bell-shaped curve was fitted through the data according to eqn (6). Using six animals, we compared the data from series 1 with those of series 2. In two of these animals we started our measurements for series 2 at P_{pa} below that at which the dynamic compliance was maximum. To fit the dynamic compliance *versus* pressure data for the second series, we used the maximum compliance obtained during the first series from the same experiment. Maximum dynamic compliance values ($C_{d,max}$) for the series at a high constant heart rate (series 2) were found at higher pulmonary arterial pressures ($P_{d,0}$) than in series 1 at an increasing heart rate (mean difference = 8·00 ± 3·28 mmHg, $P = 0{\cdot}002$, paired t test, $n = 6$, Fig. 3*Bd–i*). In series 2 at a constant heart rate, the bell-shaped curves were wider than in series 1 at an increasing heart rate, which was indicated by larger values for the width parameter ($P_{ps,1}$, eqn (6)) (mean difference = 2·11 ± 0·95 mmHg, $P = 0{\cdot}003$, paired t test, $n = 6$) (Fig. 3*Bd–i*). Panels *d*, *f*, *h* and *i* in Fig. 3*B* show that maximum dynamic compliance ($C_{d,max}$) is about the same for both series of measurements. The mean difference between $C_{d,max}$ of the first and second series is $-0{\cdot}13 \pm 0{\cdot}56$ mm^2 mmHg^{-1} (paired t test, $n = 4$, $P = 0{\cdot}689$).

DISCUSSION

Experimental conditions

In our experiments, the slightly curved conductance catheter was positioned in the centre of the pulmonary artery using radiographic imaging. The catheter did not affect the pulmonary arterial wall mechanically, thus avoiding local spasm of the vascular smooth muscle cells (Arnd *et al.* 1971). Perpendicular movement of the catheter exiting the vessel centre would cause a maximum error of 7% in the conductance signal (Woodward & Bertram, 1989). To avoid such positional changes caused by ventilatory movements we measured during prolonged expiratory pauses.

The effect of pressure

According to our data, pseudo-static compliance depends on pulmonary arterial pressure. We found a similar sigmoid relationship between the mean CSA and the mean pressure to that previously found in the aorta (Langewouters, 1984). A similar relationship applies for dynamic compliance. The compliance of the pulmonary artery is larger than that of the aorta, which we attribute to the different ratios and quantities of collagen and elastin in both vessels (Wolinsky & Glagov, 1964; Apter *et al.* 1966). According to Wolinsky

Figure 3. Pseudo-static and dynamic compliance *versus* mean pressure
A, derived pseudo-static compliance (C_{ps}, ordinate) is plotted against mean pulmonary arterial pressure (mean $P_{pa,}$ abscissa). Each panel *a–i* represents data from a single animal. Two series were done in six (*d–i*) of the nine (*a–i*) animals. The dotted line presents the first series at an increasing heart rate and the continuous line presents the second series at a constant high heart rate. *B*, for the same experiments, *a–i*, dynamic compliance (C_d, ordinate) is plotted against mean pulmonary arterial pressure (mean P_{pa}, abscissa) for a series with a changing heart rate (▲) and for a series with a constant heart rate (○). The arrows indicate the measurement taken after blood was returned to the animal but before pacing.

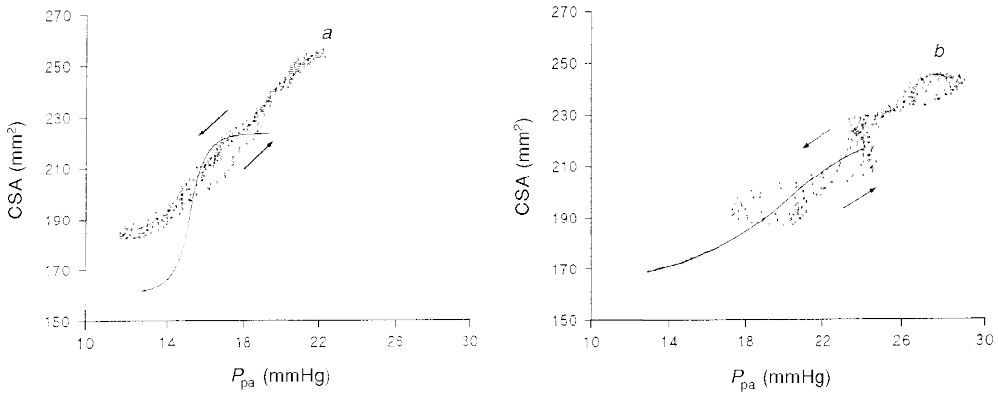

Figure 5. CSA *versus* instantaneously measured pressure over several heart cycles

The loops *a* in the left panel give the CSA *versus* instantaneously measured P_{pa} curve for the experiment shown in Fig. 2*h* when heart rate increased. For the loops *a*, mean P_{pa} is 19 mmHg, mean CSA is 226 mm^2, dynamic compliance is 7·2 mm^2 mmHg^{-1} and heart rate is 2·4 Hz. The fit through mean CSA *versus* mean P_{pa} of the first series from experiment *h* is drawn as a continuous line. The loops *b* in the right panel represent the CSA *versus* instantaneously measured P_{pa} curve for experiment *h* when heart rate was kept constant. For the loops *b*, mean P_{pa} is 24 mmHg, mean CSA is 220 mm^2, dynamic compliance is 6·0 mm^2 mmHg^{-1} and heart rate is 4·3 Hz. The fit through mean CSA *versus* mean P_{pa} of the second series from experiment *h* is drawn as a continuous line. The arrows indicate the direction of changes during a heart cycle.

and Glagov, collagen and elastin are in the folded condition at a low pressure (Wolinsky & Glagov, 1964). If pressure increases, elastin will unfold in increasing amounts and the vessel will become more compliant. When elastin unfolds, CSA becomes dependent on smooth muscle tone. At the inflection point of the sigmoid CSA *versus* pressure curve, i.e. at the pressure where the first derivative is maximum, all elastin will have unfolded, whereas the collagen will remain in a folded condition. If the stiff collagen unfolds, the distention of the vessel wall will reach its limits as characterized in the upper part of the sigmoid CSA *versus* pressure curve.

The effect of heart rate

The CSA was smaller at the same mean pulmonary arterial pressure when the heart rate was minimal than when it was controlled (Fig. 2*d*–*i*). Only when the heart rate was equal for both conditions were the CSAs equal. This was probably due to an increase in smooth muscle tone. An increase in heart rate due to bleeding might reflect an increase in sympathetic activity induced by a lower arterial pressure.

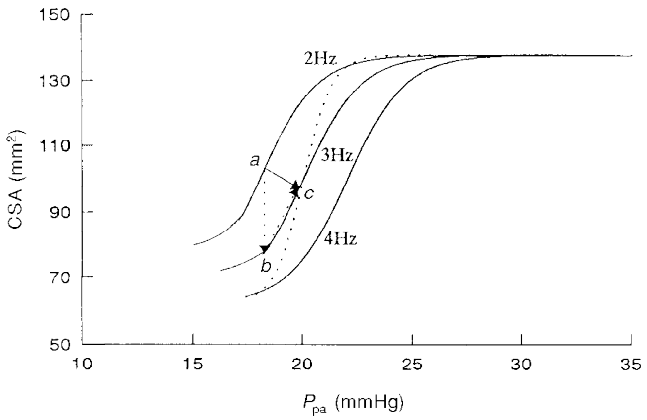

Figure 6. Schematic explanation of heart rate effects on mean CSA *versus* mean pressure relationship in the pulmonary artery

The continuous lines are cross-sectional area (CSA) *versus* pressure curves at a constant heart rate and the dashed line is a CSA *versus* pressure curve at an increasing heart rate. If, at *a*, heart rate is increased from 2 to 3 Hz the CSA will decrease and become *b*. Due to pacing, pulmonary arterial pressure will increase and the CSA will shift via the CSA *versus* pressure curve for 3 Hz and will become *c*. This procedure is repeated if the heart rate is increased from 3 to 4 Hz. If heart rate is increased in small steps the resultant curve will be the dashed line, which is steeper than the continuous line.

An increase in sympathetic activity will lead to an increase in vessel tone (Ingram *et al.* 1968). In all experiments during normovolaemia at a higher heart rate the pulmonary arterial pressure was higher and the CSA was lower than at lower heart rates. Therefore, the vasoconstriction could also be caused by the higher heart rate itself. We attributed the increase in pulmonary arterial pressure, when the heart rate was increased, to an increase in flow and/or an increase in downstream flow resistance. It is unlikely that the decrease in CSA could be explained by an increase in shear rate due to an increase in flow because shear rate would have caused vasodilatation (Melkumyants *et al.* 1994). It is likely that the rate of cyclic stretch of the pulmonary artery increases the vessel tone (Sparks, 1964; Sumpio & Widmann, 1990; Winston *et al.* 1993) as does the amount of stretch (Harder *et al.* 1987; Khalil *et al.* 1987; Kirber *et al.* 1988; Kulik *et al.* 1988; Naruse & Sokabe, 1993).

The mean CSA *versus* mean P_{pa} curve was steeper for the series where the heart rate increased than for the series where the heart rate remained constant (Fig. 2*d*–*h*). The maximum pseudo-static compliance correlated with the maximum increase in heart rate. The corresponding pressures were also correlated. We assume that these results can be explained by the model in Fig. 6, where, at various smooth muscle tones, the collagen is the limiting factor for vessel distension at high pulmonary arterial pressures. At physiological pressures the mean CSA will decrease if smooth muscle tone increases during an increase in heart rate ($a \Rightarrow b$). Furthermore, as mentioned above, an increase in pulmonary arterial pressure occurred if the heart rate increased, which caused the CSA to shift along the mean CSA *versus* mean pressure curve ($b \Rightarrow c$). Thus, we assume that the mean CSA *versus* pressure relationship at an increasing heart rate can be deduced from a population of relationships at various constant heart rates, implying that pseudo-static compliance will be overestimated if the heart rate increases. Our idea of a shift corresponds with the shift in the static diameter *versus* pressure curve found in the iliac and carotid artery during norepinephrine (noradrenaline) administration, which also caused smooth muscle contraction (Cox, 1975). The shift also corresponds with our observations that the pressure, where dynamic compliance was maximum, was highest for the series determined at a high constant heart rate and that maximum dynamic compliance did not depend on the heart rate.

Dynamic compliance

The almost closed CSA *versus* pressure loops over a heart beat indicate a negligible viscous resistance in the vessel wall, including hardly any energy being dissipated (Patel *et al.* 1960; Shelton & Olson, 1972). Furthermore, because of the closed loops, it is unlikely that the erythrocytes were reformed and de-orientated at the end of diastole.

The maximum dynamic compliance found by us ($4{\cdot}33 \pm 2{\cdot}19\ mm^2\ mmHg^{-1}$) was similar to the constant dynamic compliance of the pulmonary artery of dogs found by Patel *et al.* (1960) ($4{\cdot}94 \pm 1{\cdot}85\ mm^2\ mmHg^{-1}$), but a twofold lower compliance of the dog pulmonary artery was found by Ingram *et al.* (1970; $2{\cdot}82 \pm 1{\cdot}15\ mm^2\ mmHg^{-1}$) and Johnson & Henry (1985; $2{\cdot}25\ mm^2\ mmHg^{-1}$). In humans, a compliance of $10{\cdot}04 \pm 2{\cdot}45\ mm^2\ mmHg^{-1}$ was found by Greenfield & Griggs (1963). The differences might be dependent on differences in pressure, heart rate, vessel volume, age and species.

In summary, we conclude that the pulmonary artery constricts if the heart rate increases. Therefore, the literature on pseudo-static compliance during conditions when heart rate is changing should be reconsidered. Furthermore, we conclude that a constant dynamic compliance within a heart cycle can be used in a windkessel model because the relationship between CSA and pressure is essentially linear within a heart cycle. However, it should be noted that the effect of longitudinal compliance also needs to be studied. If a windkessel model is used to estimate flow from pulmonary arterial pressure, dynamic compliance should be determined for the corresponding haemodynamic condition (i.e. individual, heart rate and pulmonary arterial pressure). This can be attained by adding four electrodes to the pressure catheter which allow measurement of the CSA and enable the dynamic compliance to be calculated.

Apter, J. T., Rabinowitz, M. & Cummings, D. H. (1966). Correlation of visco-elastic properties of large arteries with microscopic structure. *Circulation Research* **29**, 104–121.

Arndt, J. O., Klauske, J. & Mersch, F. (1971). Mechanics of the aorta *in vivo*. *Circulation Research* **28**, 693–704.

Baan, J., Van der Velde, E. T., De Bruin, H. G., Smeenk G. J., Koops, J., van Dijk, A. D., Temmerman, D., Senden, P. J. & Buis, B. (1984). Continuous measurement of left ventricular volume in animals and humans by conductance catheter. *Circulation* **70**, 812–823.

Cox, R. H. (1975). Arterial wall mechanics and composition and the effects of smooth muscle activation. *American Journal of Physiology* **229**, 807–812.

Gozna, E. R., Marble, A. E., Shaw, A. & Holland, J. G. (1974). Age-related changes in the mechanics of the aorta and pulmonary artery of man. *Journal of Applied Physiology* **36**, 407–411.

Grant, B. J. B., Fitzpatrick, J. M. & Lieber, B. B. (1991). Time-varying pulmonary arterial compliance. *Journal of Applied Physiology* **70**, 575–583.

Greenfield, J. C. & Griggs, D. M. (1963). Relation between pressure and diameter in main pulmonary artery of man. *Journal of Applied Physiology* **18**, 557–559.

Harder, D. R., Gilbert, R. & Lombard, J. H. (1987). Vascular muscle cell depolarization and activation in renal arteries on elevation of transmural pressure. *American Journal of Physiology* **253**, F778–781.

Ingram, R. H., Szidon, J. P. & Fishman, A. P. (1970). Response of the main pulmonary artery of dogs to neuronally released *versus* blood-borne norepinephrine. *Circulation Research* **26**, 249–262.

Ingram, R. H., Szidon, J. P., Skalak, R. & Fishman, A. P. (1968). Effects of sympathetic nerve stimulation of the pulmonary artery tree on the isolated lobe perfused in situ. *Circulation Research* **22**, 801–814.

Jansen, J. R. C., Hoorn, E., van Goudoever, J. & Versprille, A. (1989). A computerized respiratory system including test functions of lung and circulation. *Journal of Applied Physiology* **67**, 1687–1691.

Jansen, J. R. C., Wesseling, K. H., Settels, J. J. & Schreuder, J. J. (1990). Continuous cardiac output monitoring by pulse contour during cardiac surgery. *European Heart Journal* **11**, 26–32.

Johnson, T. A. & Henry, G. W. (1985). Two dimensional *in vivo* pressure/diameter relationships in the canine main pulmonary artery. *Cardiovascular Research* **19**, 442–448.

Khalil, R., Lodge, N., Saida, K. & van Breemen, C. (1987). Mechanism of calcium activation in vascular smooth muscle. *Journal of Hypertension* **5**, S5–15.

Kirber, M. T., Walsh, J. V. Jr & Singer, J. J. (1988). Stretch-activated ion channels in smooth muscle: a mechanism for the initiation of stretch-induced contraction. *Pflügers Archiv* **345**, 412–345.

Kulik, T. J., Evans, J. N. & Gamble, W. J. (1988). Stretch-induced contraction in pulmonary arteries. *American Journal of Physiology* **255**, H1391–1398.

Langewouters, G. J. (1984). The static elastic properties of 45 human thoracic and 20 abdominal aortas *in vitro* and the parameters of a new model. *Journal of Biomechanics* **17**, 425–436.

Lieber, B. B., Li, Z. & Grant, B. J. B. (1994). Beat-by-beat changes of viscoelastic and inertial properties of the pulmonary arteries. *Journal of Applied Physiology* **76**, 2348–2355.

Marcus, R. H., Korcarz, C., McGray, G., Neumann, A., Murphy, A., Borow, K., Weinert, L., Bednarz, J., Gretler, D. D. & Spenzer, K. T. (1994). Noninvasive method for determination of arterial compliance using doppler echocardiography and subclavian pulse tracings. *Circulation* **89**, 2688–2699.

Melkumyants, A. M., Balashov, S. A. & Kartamyshev, S. P. (1994). Anticonstrictor effect of endothelium sensitivity to shear stress. *Pflügers Archiv* **427**, 264–269.

Naruse, K. & Sokabe, M. (1993). Involvement of stretch-activated ion channels in Ca^{2+} mobilization to mechanical stretch in endothelial cells. *American Journal of Physiology* **264**, C1037–1044.

Patel, J. D., Schilder, D. P. & Mallos, A. J. (1960). Mechanical properties and dimensions of the major pulmonary arteries. *Journal of Applied Physiology* **15**, 92–96.

Sakamoto, K. & Kanai, H. (1979). Electrical characteristics of flowing blood. *IEEE Transactions on Biomedical Engineering* **26**, 686–695.

Shelton, D. K. & Olson, R. M. (1972). A nondestructive technique to measure pulmonary artery diameter and its pulsatile variations. *Journal of Applied Physiology* **33**, 542–544.

Sómod, L., Hasenkam, J. M., Yong Kim, W., Nygaard, H. & Paulsen, P. K. (1993). Three dimensional visualisation of velocity profiles in the normal porcine pulmonary trunk. *Cardiovascular Research* **27**, 291–295.

Sparks, H. V. (1964). Effect of quick stretch on isolated vascular smooth muscle. *Circulation Research* I254–260.

Sumpio, B. E. & Widmann, M. D. (1990). Enhanced production of an endothelium-derived contracting factor by endothelial cells subjected to pulsatile stretch. *Surgery* **108**, 277–282.

Weissman, C., Ornstein, E. J. & Young W. L. (1993). Arterial pulse contour analysis trending of cardiac output: haemodynamic manipulations during cerebral arteriovenous malformation resection. *Journal of Clinical Monitoring* **9**, 347–363.

Wesseling, K. H., Jansen, J. R. C., Settels, J. J. & Schreuder J. J. (1993). Computation of aortic flow from pressure in humans using a nonlinear, three-element model. *Journal of Applied Physiology* **74**, 2566–2573.

Winston, F. K., Thibault, L. E. & Macarak, E. J. (1993). An analysis of the time dependent changes in intracellular calcium concentration in endothelial cells in culture induced by mechanical stimulation. *Journal of Biomechical Engineering* **115**, 160–168.

Wolinsky, H. & Glagov, S. (1964). Structural basis for the static mechanical properties of the aortic media. *Circulation Research* **14**, 400–413.

Woodward, J. C. & Bertram, C. D. (1989). Effect of radial position on volume measurements using the conductance catheter. *Medical and Biological Engineering and Computing* **27**, 25–35.

Acknowledgements

The authors wish to express their gratitude to A. Drop and M. van Oosterhout for technical assistance.

Corresponding author

J. R. C. Jansen: Pathophysiological Laboratory, Department of Pulmonary Diseases, Erasmus University, Room EE2251, PO Box 1738, 3000 DR Rotterdam, The Netherlands.

Email: Jansen@longz.fgg.eur.nl